
This is an electronic reprint of the original article.
This reprint may differ from the original in pagination and typographic detail.

Xie, Zichan; Wang, Haichao; Hua, Pengmin; Lahdelma, Risto

Discrete event simulation for dynamic thermal modelling of district heating pipe

Published in:
Energy

DOI:
[10.1016/j.energy.2023.129523](https://doi.org/10.1016/j.energy.2023.129523)

Published: 15/12/2023

Document Version
Publisher's PDF, also known as Version of record

Published under the following license:
CC BY

Please cite the original version:
Xie, Z., Wang, H., Hua, P., & Lahdelma, R. (2023). Discrete event simulation for dynamic thermal modelling of district heating pipe. *Energy*, 285, 1-11. Article 129523. <https://doi.org/10.1016/j.energy.2023.129523>

This material is protected by copyright and other intellectual property rights, and duplication or sale of all or part of any of the repository collections is not permitted, except that material may be duplicated by you for your research use or educational purposes in electronic or print form. You must obtain permission for any other use. Electronic or print copies may not be offered, whether for sale or otherwise to anyone who is not an authorised user.



Discrete event simulation for dynamic thermal modelling of district heating pipe

Zichan Xie ^{a,*}, Haichao Wang ^{a,c}, Pengmin Hua ^a, Risto Lahdelma ^{a,b}

^a Department of Mathematics and Systems Analysis, Aalto University, School of Science, P.O. BOX 11100, Espoo, Finland

^b Department of Mechanical Engineering, Aalto University, P.O. BOX 14100, FI-00076, Espoo, Finland

^c Institute of Building Environment and Facility Engineering, Dalian University of Technology, Dalian, 116024, China

ARTICLE INFO

Handling editor: Henrik Lund

Keywords:

Discrete event simulation
Lagrangian method
Variable time step
District heat pipe
Dynamic thermal simulation
Heat losses

ABSTRACT

Optimizing district heating (DH) systems in a holistic manner is often impeded by the computational complexities associated with network modeling. This study introduces a novel, efficient and theoretically accurate method for dynamic thermal modelling of DH pipes. The approach is to track water frontiers traveling along the pipe using discrete event simulation (DES) paradigm. As the DES method is based on variable time steps, the computational effort is significantly reduced compared to earlier methods. The proposed model can compute outlet water temperature, temperature profile along the pipe, and heat loss based on variable inlet temperature and flow rate. The DES model was validated by comparison with real measurements of a long DH pipe. Four variants of the model with different temperature profile assumptions and interpolation methods were compared. Numerical results show that the DES model can accurately predict outlet water temperature with a maximum discrepancy of 0.52 °C. The mean error of simulated outlet temperature was -0.01 ± 0.02 °C. Average computation time for 24-h simulation was 59 μ s. Overall, this study shows that the DES method is appropriate for variable time step simulation for DH pipe, potentially, for network simulation. Our study may also inspire variable time step implementation in other energy applications.

1. Introduction

In response to rising energy use and global climate change, massive efforts are being made to reduce energy consumption and emissions. Space and water heating constitutes a large share of final energy consumption in Europe [1]. Therefore, efficient heating systems are important for decarbonization [1,2]. Comparative studies on two District Heating (DH) systems have found 4th generation systems to be particularly well-suited for extensions from existing networks [3,4]. Lund et al. [5] outlines features of 4th generation DH systems aimed at minimizing losses and efficiently incorporating renewable energy. Subsequent research [6] details the necessary transformations in DH distribution networks, such as new structural layouts [7], connections with heat storages [8–10], and multiple heat sources including waste heat [11]. These upgraded networks call for intelligent network control where system optimization is important.

For planning and optimizing operation of DH systems, monitoring temperature changes is essential for implementing closed-loop control [12]; dynamic network simulation is an economical approach for

obtaining the temperature feedback [13,14]. A DH system consists of three subsystems: production, distribution network and consumers. Optimal operation of production and customer side has been extensively studied [15,16], while holistic system optimization studies involving network operation are relatively rare [17–20]. One key obstacle to such integrated studies is the lack of fast and accurate network models capable of iterative calculation [21].

It is essential that DH network models accurately simulate thermal propagation, as this is important for heat load regulation [22,23]. Two primary parameters influence thermal propagation in the network: transport time delay and heat loss. The speed of thermal propagation is approximately equal to flow speed [24], and transport time delay can vary from minutes to hours under typical operating conditions [25]. Heat loss during transmission ranges from 5 % to 20 % of the annual heat supply [13], depending on network structure, dimensions, and operating conditions. As a result, accurate calculation of thermal propagation for each pipe is imperative.

* Corresponding author.

E-mail address: xiezichan@outlook.com (Z. Xie).

<https://doi.org/10.1016/j.energy.2023.129523>

Received 10 May 2023; Received in revised form 12 September 2023; Accepted 29 October 2023

Available online 30 October 2023

0360-5442/© 2023 The Authors. Published by Elsevier Ltd. This is an open access article under the CC BY license (<http://creativecommons.org/licenses/by/4.0/>).

Nomenclature			
<i>Indices</i>		q	Heat loss rate per meter, W/m
i	Water frontier 1, 2, ...in creation and arrival order	S	Length of pipe, m
<i>Symbols</i>		s_i	Distance from the i th water frontier to the $(i-1)$ th water frontier, m
ρ	Water density, kg/m ³	t	Instance in time, simulation clock, s
τ	Time interval, travel time, s	t_{in}	Entering time of water slice, s
A	Cross section area of pipe, m ²	t_{out}	Arrival time of water slice, s
c_p	Specific heat capacity of water, J/(kg·K)	T	Water temperature, °C
E	Internal heat energy of water in pipe, J	T_{amb}	Ambient temperature, °C
E_i	Internal heat energy of water between i th and $(i-1)$ th water frontier, J	T_{in}	Inlet water temperature, °C
Q_{in}	Inlet energy, J	T_{out}	Outlet water temperature, °C
Q_{loss}	Heat loss from the water, J	v	Water flow speed, m/s
Q_{out}	Outlet energy, J	v_{out}	Outlet water flow speed, m/s
		v_{in}	Historic inlet water flow speed, m/s
		x	Distance from the pipe inlet, m

1.1. Numerical simulation approaches

In fluid mechanics, there are two methods to describe the motion of particles, Eulerian approach and Lagrangian approach. In Eulerian method, equations are established on fixed locations, where the grid is independent from particle's velocity. Compared with that, the observer is following the moving particles in Lagrangian method, which can be more efficient [26,27].

1.1.1. Eulerian approach

Eulerian approach is widely used in numerical studies due to the advantage of fixed control volumes to solve partial differential equations (PDEs). The computational burden is related to iteration steps and the complexity in each step. Therefore, scholars show big interest to search efficient solutions without iterations. Wang et al. [23] proposed a first-order implicit upwind model, which was validated by measurement data of 9.25 km pipeline from a CHP plant in China. They compared it with a model based on characteristic method [28]. The results show characteristic method is two times faster but less precise than first-order implicit upwind model. In order to improve the accuracy further, Zheng et al. [29] introduced second-order implicit upwind method and semi-implicit QUICK method, and compared those two models with the first-order method. The same experimental data was used in all three models, which showed that second-order implicit upwind method is the most efficient method with the outlet temperature error within ± 1.0 °C. Betancourt Schwarz et al. [14] developed a modified finite volume method (FVM) using the electrical analogy, which evaluated node temperatures in a network with 6 nodes. Results show that it is 3.5 times faster than a traditional FVM model, but the accuracy is related to Courant criterion. Courant criterion is a necessary condition for numerical convergence, and it requires that time step is smaller than the duration of wave traveling to adjacent grids [30].

The characteristic method, a bridge between Lagrangian and Eulerian method, has been implemented in pipe simulation for decades [12]. The principle is to convert hyperbolic partial differential equations to ordinary differential equations by manipulating Lagrangian derivative [26,30]. Combined with discretization methods, reduced energy equation can be solved efficiently. Stevanovic et al. [28,32] developed a 3rd order spatial accuracy model based on finite difference methods (FDM). It allows complex operation modeling, like bi-directional flows and zero flow speed. They tested it with measurement data from a DH network with over 50 substations. Their model performed well in rapid temperature change situation. However, they pointed out that high-order algorithm is necessary for decreasing numerical diffusion, which is incompatible with common hydraulic models [33]. Apart from that, Wang et al. [23] criticized its computation burden caused by Courant

criterion [23].

However, the accuracy of Eulerian approach is highly related to temporal discretization and spatial discretization. Models perform poorly with sharp temperature profile when coarse grids are applied [34]. Although many researchers attempted to improve the speed in solving PDEs without sacrificing accuracy, this requirement of fine grids for accurate simulation limits the computational cost reduction. Finding the appropriate settings for time step and spatial step to balance the accuracy and simulation time is also intensively researched [23,29,35], but it requires repeating work for model setting case by case. In addition, this strategy is hard to apply to network planning phase since there is no general rule for model settings.

Researchers attempted to improve accuracy in modeling sudden temperature changes under Eulerian system. A model based on total variation diminishing method with three-order resolution was validated under peak load conditions with a rapid temperature change [33]. The limitation is that Courant criterion for time step is required. Zheng et al. [36] developed an analytical model based on Fourier series expansion and compared their results with node method [31]. Both models were tested by measurement data from a DH system operated under constant flow speed. Results show that the new approach is 37 % faster than node method and has better accuracy in rapid temperature changing cases. Although they claimed that it worked well in variable flow speed cases, no further study can be found.

1.1.2. Lagrangian approach

Lagrangian method has been successfully implemented with FVM. A prominent simplified model called node method or plug-flow method, was first demonstrated in 1991 by Benonysson [31]. The idea is to track the travel time of control volume from the beginning to the end of the pipe. Variable control volume is generated when water is entering the pipe. This means that spatial discretization is determined by the water volume flow rate in each time step. Inlet average weighted water temperature determines the water temperature, which remains unchanged until the control volume leaves the pipe. The node temperature in that time step is given by the updated control volume's temperature.

A combination model of node method and analytical solution was developed later, which has similar performance on accuracy and computing speed [37]. A commercial software TERMIS [38] was developed based on the node method, without consideration of pipe material's heat capacity [39]. Detailed performance comparison of node method and TERMIS in real projects was conducted in Gabrielaitiene's studies [39,40]. Similar models can be found on TRNSYS [41]. Different from node method, TRNSYS pipe model Type 31 calculates the temperature along the pipe in every time step [42]. A modified model based on Type 31 including pipe inertia was tested with experimental data

[13]. Dénarié et al. [43] developed a model that considers the influence of boundary-layer thickness and pipe material thickness on temperature propagation. This model has been tested with experimental data from two single pipes. Additionally, they compared the performance of their model with a traditional FVM model and node method [31] by simulating temperature step response. Their findings indicate that their model is faster than traditional FVM and more accurate than node method. More recently, its performance was further confirmed in a tree-shaped network simulation with 485 pipes [44]. It is about 100 times faster than traditional FVM for a daily simulation, and for a one-year simulation, their model took about 2 h with time step at 0.25 h. Similar work in MATLAB can be found in study by Duquette et al. [35]. They concluded that 1-dimensional Lagrangian model with fixed time step can speed up the computation 4000 times compared to 1-dimensional Eulerian model with same spatial and temporal discretization setting. And spatial discretization in Lagrangian model has a minimal influence on accuracy. Similar work can be found in a Modelica-based framework [45]. MATLAB based models replaced uniform temperature in each cell with a linear profile by tracking the temperature changes of cells' interface [27,46].

These Lagrangian FVM models are more flexible and accurate than models based on Eulerian method because of flexible spatial discretization. However, numerical error due to fully mixed outlet temperatures in each time step cannot be avoided. To amend this problem, pipe simulation using Lagrangian method with infinitesimal segment was investigated and can be found in few studies. In Modelica environment, there is a built-in operator named `spatialDistribution` for sampling, linear interpolation, and shifting the stored distribution [47]. This operator can be used for time tracking and temperature tracking. It is capable of handling zero and reversal flow in DH pipes. A pipe model of IBPSA Modelica Library was implemented based on `spatialDistribution`, and tested by van der Heijde [48]. Results show that dynamic thermal simulation is accurate and fast using steady-state heat loss function. The pipe model in `DistrictHeating` Modelica library has similar implementation [49]. However, due to using `spatialDistribution`, updating of the values for all sampling points is required in each time step, which may cause computational burden for large-scale simulation.

1.2. Research gap

Numerous studies highlight the advantages of Lagrangian models over Eulerian models in terms of accuracy and computational speed. Among these Lagrangian models, the infinitesimal segment method has shown particular promise for achieving accurate simulations even with coarser spatial grids. But some scholars prefer FVM over infinitesimal segment method due to concerns about potential numerical instability [45].

Theoretically, infinitesimal segment method could simulate temperature propagation with variable time steps. The gap in current research lies in the overlooked potential of variable time steps for DH system simulation. This oversight has hindered the development of faster and more accurate dynamic simulations [50]. Specifically, there is a need to establish a theoretical foundation for the accurate and stable implementation of variable time steps in DH system simulations, as well as to identify a suitable simulation methodology that can efficiently execute this approach.

1.3. Novelty

Our study introduces several novel contributions to the arena of District Heating (DH) system modeling. Foremost among these is that we introduce theoretically sound conditions for thermal simulation in infinitesimal segment modeling. Building upon this theoretical foundation, we develop a Lagrangian DH pipe model that employs variable time steps implemented in C++. Notably, this is the first research to apply Discrete Event Simulation (DES) [51] in DH pipe simulation.

Our DES model considers heat loss and time delay of water traveling in a pipe. It efficiently and accurately manages variable inlet temperatures and flow rates including zero flow rate. This paper presents the detailed calculation of temperature propagation in a pipe. The proposed model is validated using measurement data, offering the following advantages:

- (1) Variable temporal and spatial discretization determined automatically by input data.
- (2) No numerical diffusion regarding the transport time delay and temperature.
- (3) Fast computation of heat loss and temperature drop.

2. Methodology

The temperature propagation calculation is based on plug flow model, where uniform velocity is assumed for all cross-sections of the pipe. For fast computation, the difference between thermal frontier and hydraulic frontier is neglected. The impact of replacing temperature wave speed with water flow speed has been discussed in Refs. [24,25,52]. As a result, accurately predicting particles' travel time is significant in studying the temperature waves caused by fluid motion.

Regarding the effects of heat transmission, constant ambient temperature is assumed for heat loss calculation. Heat gain due to friction between pipe wall and water is ignored. Additionally, axial heat transmission is not considered because it is negligible in forced flow. With these assumptions, heat loss of water particles is related to particles' travel time, temperature difference between water and ambient, and overall heat transfer coefficient. In the following, we present the DES implementation in section 2.1. A theoretically accurate approach to simulate water particles' travel time is proposed in section 2.2. Both accurate and simplified approaches for water temperature modeling are described in section 2.3. Heat loss calculation is described in section 2.4.

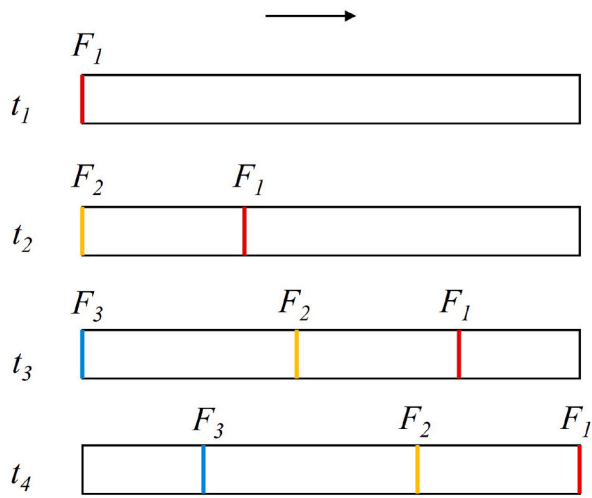
2.1. Discrete event simulation modeling

The main idea of discrete event simulation (DES) is to simulate parallel processes as a sequence of events. An event can be considered as a state change. Events can be scheduled, rescheduled, and cancelled during the simulation. The occurrence order is handled by an *event queue* with events ordered according to their scheduled activation time. Different from time-driven simulation method with fixed time steps, in DES the simulation time jumps from current event time to the next event time, which means that the time steps depend on the activation of events, and therefore they are of variable length.

The pipe simulation is based on tracking how water frontiers travel in the pipe. A *water frontier* is an infinitely short section of water traveling in the pipe assuming plug flow. The DES model includes three types of events: inlet temperature change, flow rate change and water frontier arrival at end of pipe. Inlet temperature change events and flow rate change events may occur independently, given by input data. Water frontier arrival events will be generated during the simulation. Flow rate remains constant between two flow rate change events.

Water frontiers are created at the inlet of the pipe when either inlet temperature changes or flow speed changes. The water frontiers travel through the pipe until they arrive at the outlet, which constitutes the arrival event. The sequence of water frontiers is managed by a First-In-First-Out (FIFO) queue. The water frontier to reach the outlet first, is called the *first frontier*, while the most newly created is the *last frontier*. Initially, the queue is empty, and the pipe is initialized into steady-state operation based on constant flow rate and inlet temperature. When the FIFO queue is non-empty, the arrival event of the first frontier is always scheduled in the event queue. The activation time of the arrival event is computed when a frontier reaches first position, and it is updated whenever the flow rate changes.

Fig. 1 demonstrates this method with a simple example including



Initial condition: inlet temperature is T_1 and flow speed is v_1

- t_1 : Inlet temperature increases from T_1 to T_2
- t_2 : Flow speed increases from v_1 to v_2
- t_3 : Flow speed decreases from v_2 to v_3
- t_4 : Water frontier F_1 arrives at the pipe end

Fig. 1. DES schematic diagram of an example.

four events, one inlet temperature change at t_1 , two flow speed changes at t_2 and t_3 , and one water frontier arrival at t_4 . Fig. 2 shows the corresponding state changes.

- At t_1 , inlet temperature changes, the first and only frontier F_1 is created, and corresponding arrival event is scheduled based current flow rate (flow speed).
- At t_2 , flow rate changes, a second water frontier F_2 is created, and the arrival time of F_1 is recomputed based on the new flow speed.
- At t_3 , flow rate changes again, water frontier F_3 is created and arrival time of F_1 is recomputed.
- At t_4 , frontier F_1 arrives, and it is removed from the FIFO queue. F_2 becomes the first frontier, and it is scheduled to arrive based on current flow rate.

2.2. Travel time calculation

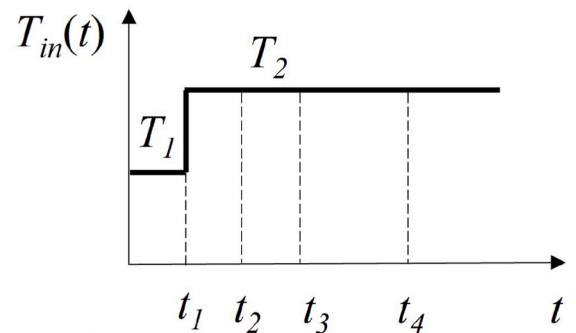
Travel time of water particles depends on the variable flow speed that they experience during their journey through the pipe. Flow speed v at given time is computed from the mass flow rate \dot{m} based on cross-section area A of the pipe and constant density of water ρ .

$$v = \dot{m} / (\rho A) \quad (1)$$

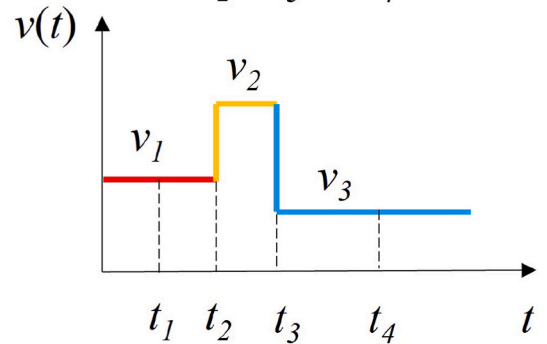
Travel time τ of each particle is the difference between the arrival time t_{out} and entering time t_{in} :

$$\tau = t_{out} - t_{in} \quad (2)$$

For a water frontier, t_{in} is its creation time, and t_{out} is its arrival time. The arrival of the first frontier is always scheduled in the event queue at the expected arrival time. Assuming flow speed $v > 0$, the expected arrival time of the first frontier is computed as



(a)



(b)

(c)

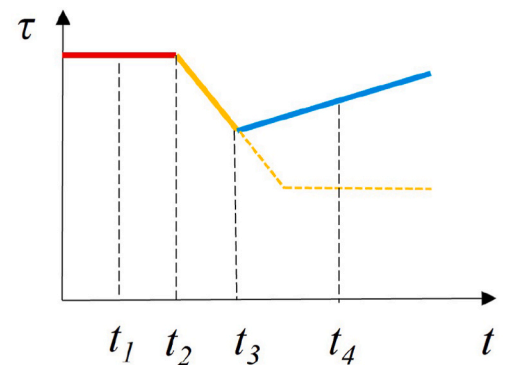


Fig. 2. State changes of an example: (a) inlet temperature profile; (b) water flow speed profile; (c) transport time delay profile.

$$t_{out} = t + s_i / v \quad (3)$$

where s_i is the remaining travel distance of the frontier. When a water frontier i is created, s_i is defined as the distance to the previous $(i-1)^{th}$ water frontier if it exists. If no previous water frontier exists, s_i is set to pipe length S . We note that this distance does not change until the frontier reaches the first position in FIFO queue. A water frontier becomes first either after the previous frontier has arrived or if the FIFO queue is empty when the frontier is created. When the i th water frontier becomes the first, its remaining distance to the outlet is equal to s_i .

The arrival time needs to be updated when the flow speed changes. The new arrival time t_{out}' is given by the following, where v' refers to the new flow speed.

$$t_{out}' = t + (t_{out} - t)v / v' \quad (4)$$

A notable fact is that the travel time $\tau(t)$ of the particles arriving at the outlet at time t is a piecewise linear function, as illustrated in Fig. 2 (c). Furthermore, travel time function is continuous as long as flow is positive. The proof is given below. For an arbitrary particle, the integral of its experienced speed over travel time equals pipe length. In Eq. (5), t_{out} and t_{in} refer to the water frontier that has left the pipe, while t_{out}' and

t_{in}' refer to the particle which arrives at outlet at the current simulation time, where $t_{in} < t_{in}' \leq t_{out} < t_{out}' = t$.

$$S = \int_{t_{in}}^{t_{out}'} v(t)dt = \int_{t_{in}'}^{t_{out}'} v(t)dt = \int_{t_{out}}^{t_{out}'} v(t)dt + \int_{t_{in}}^{t_{out}} v(t)dt - \int_{t_{in}}^{t_{in}'} v(t)dt \quad (5)$$

It implies that the integral of particles' historic inlet speeds from t_{in} to t_{in}' is the same as the integral of particles' arriving speeds from t_{out} to t_{out}' . Since inlet speed of particles between two adjacent water frontiers are constant, as mentioned in section 2.1, we get the following equation when the flow speed holds between t_{out} and t_{out}' .

$$t_{in}' = t_{in} + (t_{out}' - t_{out})v_{out} / v_{in} \quad (6)$$

Taking the case in Fig. 1 as an example, the two grey areas in Fig. 3 are the same, and v_3 and v_1 represent v_{out} and v_{in} , respectively.

τ' can be calculated based on a reference travel time τ , which has been computed by water frontier's arrival time subtracted by creation time. Based on the derivation from Eq. (7), travel time between two moments is a linear function when speed ratio does not change. The slope of the linear function is related to the particles' historic inlet speed and current speed, and the slope is constant when the speed ratio is fixed. Although this formula is derived for positive flow speed, it also applies to zero flow ($v_{out} = 0$).

$$\begin{aligned} \tau' &= t_{out}' - t_{in}' = t_{out}' - t_{in}' - \tau + \tau = t_{out}' - t_{in}' - (t_{out} - t_{in}) + \tau \\ &= (t_{out}' - t_{out}) - (t_{in}' - t_{in}) + \tau = \left(1 - \frac{v_{out}}{v_{in}}\right)(t_{out}' - t_{out}) + \tau \\ &= \tau + \left(1 - \frac{v_{out}}{v_{in}}\right)\Delta t \end{aligned} \quad (7)$$

To conclude, updating reference travel time and the slope is necessary at the water frontier arrival moments, and at breakpoints when flow speed changes during two water frontier arrival events. Even if the water frontier created by inlet temperature change does not affect the slope, reference travel time and slope will be recalculated when the water frontier arrives due to equal treatment of all water frontiers.

Consequently, travel time between two arrival events is a linear function when the flow speed remains constant between the events. Changes in flow speed make the travel time a piecewise linear function throughout the simulation time. Travel time function is continuous when flow speed is positive. Zero flow speed creates non-continuous jumps in the travel time function.

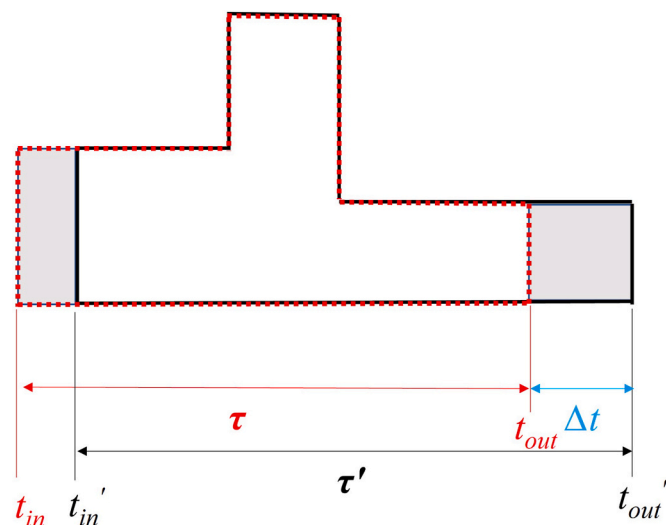


Fig. 3. Travel distance as integral of travel speed over time.

2.3. Temperature calculation

Eq. (8) gives energy balance equation assuming constant water density ρ and specific heat capacity c_p , without consideration of hydraulic effects and axial heat diffusion. On the left side, there are derivative terms of internal heat energy with respect to time t and location x . The right-hand side is the heat loss rate $q(t,x)$. Positive $q(t,x)$ denotes the heat transfer from water to the environment.

$$\rho c_p A \frac{\partial T(t,x)}{\partial t} + \rho c_p A v \frac{\partial T(t,x)}{\partial x} = -q(t,x) \quad (8)$$

In Lagrangian approach, spatial coordinate is missing because observer follows moving particles [26]. Total thermal resistance R from water to environment is used in heat loss calculation to avoid iterative calculation for different layers. Eq. (8) can be simplified into

$$\begin{aligned} \rho c_p A \frac{dT}{dt} &= -\frac{T - T_{amb}}{R}, \text{ or equivalently} \\ \frac{1}{T - T_{amb}} dT &= -\frac{\rho c_p A}{R} dt. \end{aligned} \quad (9)$$

T_{amb} is ambient temperature, which can be ambient air temperature or ground temperature. Integrating Eq. (9) from inlet state to outlet state gives the outlet temperature Eq. (10). T_{out} is the particle's current temperature when the particle reaches the outlet after travel time τ .

$$T_{out} = T_{amb} + (T_{in} - T_{amb})e^{-\frac{\tau}{\rho c_p AR}} \quad (10)$$

Hence, particle's temperature in the pipe is an exponential function of time asymptotically approaching ambient temperature, as shown in Fig. 4.

Eq. (10) and further formulas are simplified when we express temperatures in relation to ambient temperature, i.e. shift the temperature scale so that $T_{amb} = 0$ and introduce negative constant $C = -1/(\rho c_p AR)$. Then

$$T_{out} = T_{in} e^{C\tau} \quad (11)$$

Assuming that the inlet temperature is exponential function of t (or constant as a special case), also outlet temperature is exponential function of t when $\tau(t)$ changes linearly. As a result, the outlet temperature will be a piecewise exponential function of t , with breakpoints matching the breakpoints of the piecewise linear travel time function

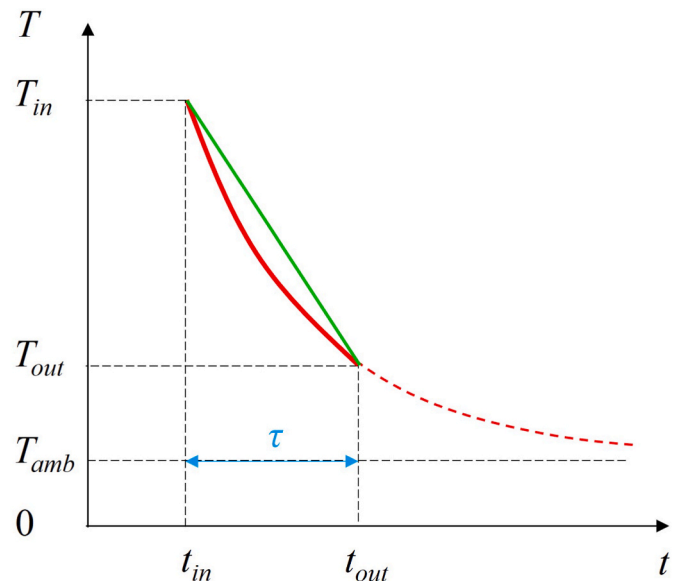


Fig. 4. One particles temperature profile when it travels through the pipe (red line: exponential profile; green line: linear approximation).

$\tau(t)$.

We introduce two coefficients k and α , for exponential interpolation of inlet temperature. The initial k and α are found by solving system of two equations based on adjacent inlet water frontiers. Inlet temperature across time t is a piecewise exponential function, and the function between two breakpoints can be described as Eq. (12). t_{in}^* refers to the previous inlet temperature change event time, which is a given constant for each inlet exponential function between two inlet temperature change events. The inlet temperature between two breakpoints is a convex function when inlet temperature is above ambient temperature.

$$T_{in}'(t) = ke^{\alpha(t-t_{in}^*)} \quad (12)$$

Combining equations (6), (7), (11) and (12), we get Eq. (13) for outlet temperature between two adjacent breakpoints. Similarly, the reference historic water frontier's inlet speed (v_{in}) is based on previous arrived water frontier. Since k and α need to be updated after water frontier arrival, the coefficients α' and β' will be calculated. Additionally, two coefficients of outlet temperature will be recalculated when flow speed changes due to the change of the reference outlet speed (v_{out}), outlet time (t_{out}) and travel time (τ).

$$T_{out}'(t) = ke^{\alpha'(t-t_{out})+\beta'} \quad (13)$$

$$\begin{cases} \alpha' = (\alpha - C) \frac{v_{out}}{v_{in}} + C \\ \beta' = \alpha(t_{out} - t_{in}^*) + (C - \alpha)\tau \end{cases}$$

For comparison, linear interpolation is also applied to compute the temperature between two adjacent breakpoints. Linear approximation is reasonable when the exponential function is nearly linear, i.e., when the temperature drop is small.

We define two alternative modes for representing inlet temperature profile within the time intervals $[t_i, t_{i+1}]$.

- The *instant mode* means that inlet temperature changes immediately at given instance of time t_i and remains at that temperature until next temperature change at t_{i+1} . This means that inlet temperature profile is a step function.
- The *gradual mode* means that inlet temperature changes gradually within each time interval. Inlet temperature profile is a piecewise exponential function when exponential interpolation is used, while it is a piecewise linear function under linear interpolation.

2.4. Heat loss

Heat loss can be calculated directly by temperature drop of particles, or indirectly by energy balance. We choose energy balance method as displayed in Fig. 5, where the reference temperature is ambient temperature. Heat loss calculation is an optional function in this model. Heat loss can be computed for an arbitrary period.

Heat loss from water to environment between t_0 and t_{end} is given by the equations (14)–(17). The right-hand side terms of Eq. (14) represent the inlet energy, outlet energy and internal energy change. Inlet energy (Q_{in}) and outlet energy (Q_{out}) are accumulated variables, which are updated during the simulation. Q_{in} and Q_{out} can be updated separately,

which makes computation more efficient. Q_{in} is updated when new water frontier is generated, while Q_{out} is updated at breakpoints of outlet temperature function. Internal heat energy $E(t)$ is a state variable, which is only calculated at t_0 and t_{end} .

$$Q_{loss} = \int_{t_0}^{t_{end}} \int_0^S q(x,t) dx dt = Q_{in} - Q_{out} - (E(t_{end}) - E(t_0)) \quad (14)$$

$$Q_{in} = \rho c_p A \int_{t_0}^{t_{end}} v(t) T_{in}(t) dt \quad (15)$$

$$Q_{out} = \rho c_p A \int_{t_0}^{t_{end}} v(t) T_{out}(t) dt \quad (16)$$

$$E(t) = \rho c_p A \int_0^S T(t,x) dx \quad (17)$$

Since energy calculation is based on ambient temperature, Eq. (12) and Eq. (13) can be applied in Eq. (15) and Eq. (16). Due to constant flow speeds between breakpoints, the integrands in Eq. (15) and Eq. (16) are piecewise exponential functions, whose breakpoints match temperature functions' breakpoints. Therefore, we break integration for Q_{in} and Q_{out} into pieces, and the integration between two breakpoints is given by Eq. (18) and Eq. (19), respectively. Here, t_{in} refers to the creation time of previously created water frontier, while t_{out} is the arrival time of previously arrived water frontier. t_{in}^* and t_{in} have the same value when the previously created water frontier is created by inlet temperature change event. α' and β' were defined in Eq. (13).

$$Q_{in} = \rho c_p A k v \left(e^{\alpha(t-t_{in}^*)} - e^{\alpha(t_{in}-t_{in}^*)} \right) / \alpha \quad (18)$$

$$Q_{out} = \rho c_p A k v e^{\beta'} \left(e^{\alpha'(t-t_{out})} - 1 \right) / \alpha' \quad (19)$$

Similarly, temperature profile in the pipe at arbitrary time t is a piecewise exponential function of distance from pipe inlet x . This allows computing integral Eq. (17) in pieces. The internal heat energy between water frontier i and $i-1$ is given by the following equation where t_{in}^i is the creation time of water frontier i , and $t_{in}^{(i-1)*}$ is the activated time of the latest inlet temperature change event when water frontier $i-1$ was created. When water frontier $i-1$ is the last (frontier i does not exist), t_{in}^i is equal to time t and s_i is distance from the inlet to the last water frontier. When water frontier i is the first, s_i is its remaining distance to the outlet.

$$E_i(t) = \rho c_p A k e^{\lambda} \left(e^{\gamma s_i} - 1 \right) / \gamma \quad (20)$$

$$\begin{cases} \gamma = (C - \alpha) / v_{in} \\ \lambda = (\alpha - C) t_{in}^i + Ct - \alpha t_{in}^{(i-1)*} \end{cases}$$

In linear interpolation, inlet temperature is assumed to be a piecewise linear function of t , and outlet temperature profile is approximated by piecewise linear function. Because flow rate is constant between two breakpoints, integration in Eq. (15) and Eq. (16) are simplified due to

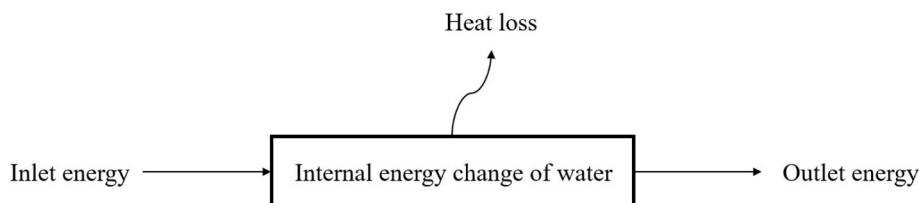


Fig. 5. Energy balance of pipe during simulation.

linear integrands. For computing internal heat energy, the water temperature profile across location x from inlet to outlet is needed. The water frontier's temperature can be calculated as in Eq. (11), but the traveling time so far of each water frontier is calculated by simulation time t minus water frontier's creation time. Water temperature profile as function of location x is also approximated by a piecewise linear function.

3. Model testing and validation

We test and compare four variants of the model:

- *instant* inlet temperature with exponential interpolation (IE),
- *instant* inlet temperature with linear interpolation (IL),
- *gradual* inlet temperature with exponential interpolation (GE), and
- *gradual* inlet temperature with linear interpolation (GL).

The models are tested and validated with 24-h measured inlet temperature, outlet temperature and flow rate data for a long DH pipe in Shijiazhuang, China [23]. The inlet temperature varies from 88.4 °C to 97.9 °C, while the flow rate changes between 9012.4 and 9761.8 m³/h. The measurement time step is 5 min, with the accuracy of temperature sensor of ± 0.4 °C, and accuracy of flow meter of 0.01 m³/h [29]. According to the extracted data, there are 256 inlet temperature change events and 258 flow rate changes events given as input to our models. The inlet temperature and flow rate are shown in Fig. 6 and other parameters in Table 1. The initial state of the pipe is unknown, but we assume steady state operation at the first measured inlet temperature of 88.5 °C and flow rate of 9761.8 m³/h.

3.1. Model validation

Fig. 7 displays the measured and simulated outlet temperatures. The red shaded area before 1.58 h shows initialization period until the first water frontier arrives at outlet. The results demonstrate that, despite the measured temperature pattern being a little smoother than simulated patterns, all four models show good agreement with measured outlet temperature apart from the initializing phase. A little larger gap between models with different inlet temperature mode can be seen when the temperature changes sharply.

The difference between the models with linear or exponential interpolation is negligible in terms of outlet temperature prediction.

Table 1
Parameters of the transient models for the investigated pipe [23].

Parameters	Values	Parameters	Values
Pipe Length (S)	9250 m	Pipe inner diameter	1400 mm
Water specific heat capacity (c_p)	4200 J/(kg·K)	Water density (ρ)	960 kg/m ³
Total thermal resistance (R)	0.35 m·K/W	Ambient temperature (T_{amb})	-10 °C

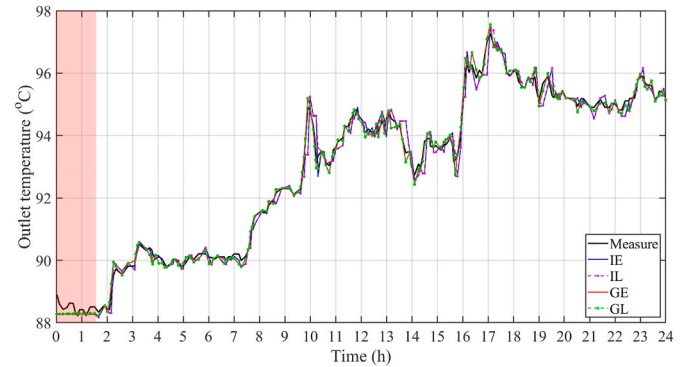


Fig. 7. Comparison of measured and simulated outlet temperatures.

Although the predicted outlet temperatures by different interpolation methods start deviating when the flow speed changes between two *arrival* events, this deviation will be reset when a new water frontier arrives. Therefore, the deviation is insignificant when water frontiers are close to each other.

Fig. 8 shows statistical outlet temperature errors of our models based on 199 measured samples (excluding initializing period). *Gradual mode* models' error distributions are narrower, and they follow normal distribution (tested by One-Sample Kolmogorov-Smirnov Test at 5 % significance level). As the impact of interpolating approaches is marginal, the curves of GL and GE are almost overlapping. The maximum error of *gradual mode* models is ± 0.6 °C, while is up to ± 1.6 °C for *instant mode* models. The mean errors and sample standard deviations are listed in Table 2. According to the accuracy indicators, *gradual mode* models (GL and GE) perform better. On average, among all four models, the simulated temperatures are slightly lower than measurements, which might

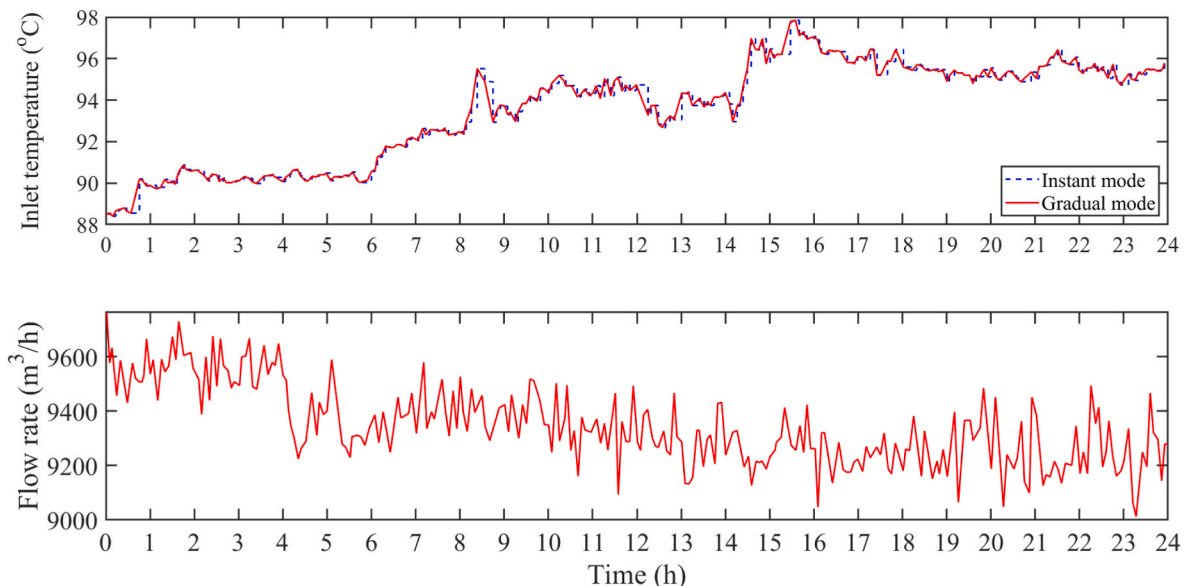


Fig. 6. Input data (top: inlet temperature; bottom: flow rate) [23].

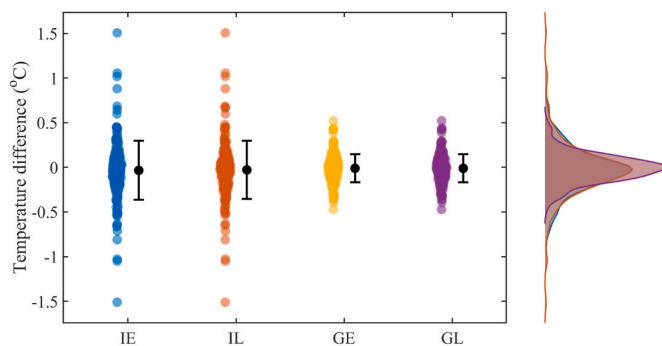


Fig. 8. Outlet temperature prediction errors of four models.

Table 2

Accuracy indicators for outlet temperature prediction across four models (unit: °C).

Models	IE	IL	GE	GL
Mean Error	-0.03	-0.03	-0.01	-0.01
Sample Standard Deviation	0.33	0.33	0.16	0.16
95 % Confidence Interval	[-0.08,0.01]	[-0.07,0.02]	[-0.03,0.01]	[-0.03,0.01]

be caused by slight overestimation of heat loss.

Fig. 9 shows the temperature error of the GL model. Excluding initialization, the maximum error is 0.52 °C. Besides, the temperature error is within ± 0.5 °C. This is comparable with characteristic line method and implicit upwind method [23], and better than first-order implicit upwind method, two iteration-free numerical methods with high-order precision [29].

3.2. Energy balance

Heat loss estimation is important for economical DH network design. Although we have discussed the differences in outlet temperature prediction among four models in section 3.1, it is worth investigating the differences from the energy side since the deviation of energy calculation will accumulate during simulation. Table 3 summarizes the energy results calculated from 0 to 24 h, including internal heat energy at 0 h and 24 h, internal heat energy changes, total inlet energy, total outlet energy, heat loss, and the ratio of heat loss to inlet energy.

Table 3 indicate that neither the interpolation method nor the inlet temperature assumption affects energy computation significantly. This can be explained by the fact that, in comparison to the absolute temperature above ambient temperature, the temperature difference between the models is very small. The estimated heat loss for linear interpolation models is slightly lower than that for exponential

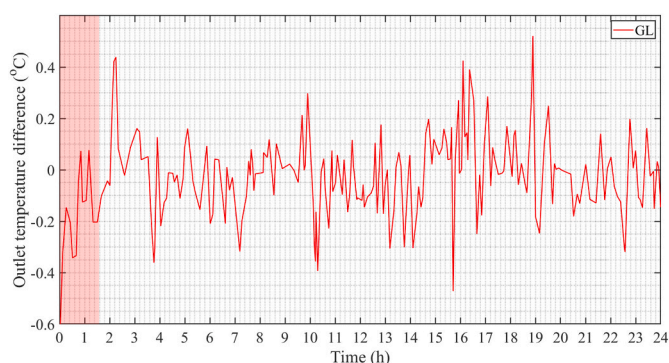


Fig. 9. Outlet temperature difference between measurements and GL model.

interpolation models. Linear approximation results in larger energy estimations compared to exponential approximation when temperature profiles are piecewise convex. The difference in heat loss caused by linear interpolation will be partly balanced out because the inlet and outlet temperature profiles for exponential models are piecewise convex (Fig. 4).

3.3. Temperature profile along the pipe

Although these models aim to predict the node temperature, they can provide temperature profile along the pipe at any time when detailed calculation is requested. Taking GL model as an example, Fig. 10 visualizes the temperature profiles at 9:00 and 9:30. In 30 min the temperature profile has advanced about 3053 m and cooled down a little (less than 0.1 °C).

Temperature profiles are simulated by 28 water frontiers in the FIFO queue at 9:00, and 29 at 9:30. Fig. 10 shows the possibility to delete water frontiers when they have little effect on the profile. Deleting such redundant water frontiers may speed up the computation significantly in large models. Criteria for deleting redundant frontiers is a topic for future research.

3.4. Computational speed

We tested the computation time needed for a 24-h outlet temperature simulation using the presented four variants of the model. The evaluations were carried out in Microsoft Visual Studio on a laptop with an Intel Core i7-1185G7 CPU @ 3.00 GHz processor.

GL model was the fastest, recording an average computation time of 59 μ s over 1000 tests. The comparative average computation times standardized to the GL model's time are detailed in Table 4.

As we can see, the impact of interpolation methods on computation time is relatively small compared to the impact of inlet temperature assumption. Despite both the GL and GE models having the same number of water frontiers, standing at 505, opting for linear interpolation instead of exponential interpolation results in a 10 % reduction in simulation time. This efficiency is attributed to the simpler calculations in linear interpolation. In linear interpolation, there is no requirement to update additional coefficients at each step, as is the case with exponential interpolation. Furthermore, choosing *gradual mode* instead of *instant mode* can speed up the simulation 24 % (IL and GL). 759 water frontiers were created in instant models as two attached water frontiers (the distance between frontiers is zero) were needed at every inlet temperature change event.

In summary, while determining the optimal approach for simulations, a pivotal factor to consider is the total number of water frontiers being tracked, as it is directly proportional to the simulation time. However, given that the computation time in a compact test can be sensitive to various factors, the speed test in a single pipe simulation may not fully demonstrate the advantage of DES model. Computational speed test of DES model in an entire network should be conducted in future studies.

4. Discussion

Our study represents an efficient and accurate solution for pipe modelling. In the test pipe simulation, DES model generated 505 water frontiers and simulated 986 outlet temperature sampling points. However, classic Eulerian models need significantly higher computational resources to achieve a comparable level of temperature accuracy for the same simulation [23]. Compared with the number of water frontiers generated, the control volumes required by the optimal characteristic line model were approximately three times more, and these needed for the optimal implicit upwind method were about nine times more. In terms of temperature sampling points, DES model computed roughly 29 and 1350 times fewer temperature sampling points, respectively. As a

Table 3
Energy calculation across four models (unit: MWh).

Models	$E(t_0)$	$E(t_{end})$	$E(t_{end}) - E(t_0)$	Q_{in}	Q_{out}	Q_{loss}	$Q_{loss}/Q_{in}(\%)$
IE	1569.19	1676.68	107.48	26011.09	25837.99	65.62	0.25
IL	1569.19	1676.83	107.64	26011.09	25837.99	65.47	0.25
GE	1569.19	1677.12	107.92	26014.80	25841.30	65.57	0.25
GL	1569.19	1677.22	108.02	26014.81	25841.56	65.23	0.25

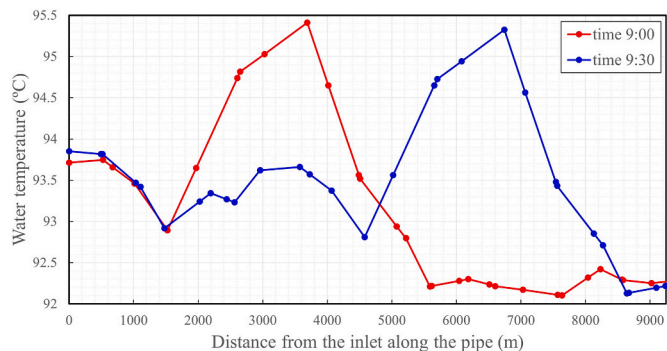


Fig. 10. Water temperature profiles along the pipe calculated by model GL.

Table 4
Standardized average computation time based on GL model.

Models	IE	IL	GE	GL
Standardized computation time	1.42	1.31	1.11	1

result, the DES model is 593 and 1288 times faster than the aforementioned methods, respectively. While a recent study applied the implicit upwind model in mesh DH system optimization, the authors conceded its impracticability in engineering applications, primarily due to the extensive computation time consumed by thermal calculation [19]. DES model has the potential to simulate large-scale networks efficiently, possibly paving the way for feasible DH system optimization.

The proposed GE and GL models assuming gradual change of inlet water temperature between the measurements basically performed equally well in outlet temperature prediction. Also, the gradual temperature change models performed better than the instant mode models (IE and IL). There are two possible reasons for this result. First, the gradual temperature change assumption may represent the experimental setup and practical operation of DH networks more accurately than the *instant mode*. Second, the *gradual mode* results into smoother temperature profile (outlet standard deviation in Table 2), matching better with measurements. Axial heat transmission makes the measured outlet temperature profile smoother, but this impact is overlooked in the water frontier model.

While the two gradual models exhibit comparable performance in predicting temperature, the GL model has the advantage of requiring less computation time. This illustrates that pinpointing the breakpoints of the temperature profile is an efficient strategy. Furthermore, although the simulation presently employs fixed water properties and ambient temperature, the linear models are designed to be more flexible and capable of adjusting to variable parameters throughout the simulation. For example, the viscosity and density of water that depend on water temperature can be defined separately for each water frontier. This feature positions the GL model as a more suitable option for long-term, large-scale network simulations, where constant parameter assumption may be an issue. Further improvements should focus on linear models, unless new theories for exponential models can support wider applications.

Our method offers the benefit of relating temperature accuracy to

input data frequency rather than spatial discretization. It is possible to fully apply the given information without generating numerical errors. Yet, in some circumstances, this method might lead to distorted temperature profiles. It can explain why the predicted temperature is more fluctuating compared to measurements. Apart from that, the influence of pipe wall's thermal inertia is ignored in this study. Although there is a study claiming that this simplification has a minor influence on the pipes with large diameters [33], this model has the possibility to consider the effect of pipe wall thermal inertia when it is extended to network simulation. Two possible ways allow investigating the impact in our model. One approach is to assume uniform pipe wall temperature for each pipe as in many previous studies [23,31,37,43,48]. The other approach is to assume infinitesimal thermal resistance between water and steel as [52]. To conclude, the approaches to smoothing temperature profiles are expected in future work for accuracy improvement.

5. Conclusion

This study proposed a novel and theoretically accurate discrete event simulation approach to dynamic thermal simulation of DH pipes. The method is based on tracking water frontiers traveling in the pipe by discrete event simulation. It is an accurate, numerically stable, flexible, and computationally efficient solution for calculating temperature propagation in pipes. Inlet temperature was assumed to change either instantly (I), or gradually (G) between measurements. Linear (L) and exponential (E) interpolation were adopted to compute water temperature between frontiers. The accuracy of the four different models (IE, IL, GE, GL) was validated by comparing the simulated outlet temperatures against real measurements for a 9250 m long pipe. The results showed that:

- (1) Simulated temperatures from GL and GE models show strongest agreement with the measurements with mean error -0.01 °C and standard deviation 0.16 °C.
- (2) The inlet temperature profile has a significant influence on temperature simulation. *Instant mode* can be useful when the average temperature is given, for example, when a pipe is connected with heat storage. Otherwise, *gradual mode* should be chosen.
- (3) Using the linear or exponential interpolation approach barely impacts the temperature prediction and heat loss estimation.
- (4) GL model is the accurate and efficient, which can complete the 24-h simulation within 59 μ s.
- (5) The DES pipe model with variable time steps is efficient and flexible. The model is promising for large-scale DH networks simulation.

It is noteworthy that although our method aims at node temperature computing, it preserves the ability to simulate the temperature profile along the pipe, which facilitates further development for mesh DH networks. Future research should implement and test the DES approach on entire DH networks. It remains to be validated if the efficiency of the method is sufficient also for large networks, or if the number of water frontiers in deep network branches slows down the computation. One possibility to reduce the number of water frontiers is to delete redundant water frontiers not affecting the temperature profile significantly. This implies a tradeoff between computation speed and accuracy in temperature calculations.

Additionally, the DES methodology is not limited to DH networks; it holds potential for broader applications in other industries. With minor adaptations, this technique could be applied in sectors, including but not limited to district cooling system, oil delivery systems, water distribution networks, and even thermal storage simulation. Researchers in these domains may find it beneficial to explore the applicability of DES, as it could significantly contribute to future cross-sector energy system simulation with variable time steps.

CRedit authorship contribution statement

Zichan Xie: Conceptualization, Methodology, Software, Validation, Investigation, Data curation, Visualization, Writing – original draft, Writing – review & editing. **Haichao Wang:** Funding acquisition, Writing – review & editing. **Pengmin Hua:** Writing – review & editing. **Risto Lahdelma:** Supervision, Conceptualization, Methodology, Software, Writing – review & editing.

Declaration of competing interest

The authors declare that they have no known competing financial interests or personal relationships that could have appeared to influence the work reported in this paper.

Data availability

The authors do not have permission to share data.

Acknowledgements

This study was supported by academy research fellow funding from Research Council of Finland (Funding No. 334205 and 358055).

References

- [1] European Commission. Directorate General for Energy, E-Think, TU Wien, Fraunhofer ISI, Öko Institut e.V, Viegand Maagoe. Renewable space heating under the revised Renewable Energy Directive: ENER/C1/2018 494 : final report. Luxembourg: Publications Office of the European Union; 2022.
- [2] Su L, Nie T, On Ho C, Yang Z, Calvez P, Jain RK, et al. Optimizing pipe network design and central plant positioning of district heating and cooling System: a Graph-Based Multi-Objective genetic algorithm approach. *Appl Energy* 2022;325:119844. <https://doi.org/10.1016/j.apenergy.2022.119844>.
- [3] Lund H, Østergaard PA, Nielsen TB, Werner S, Thorsen JE, Gudmundsson O, et al. Perspectives on fourth and fifth generation district heating. *Energy* 2021;227:120520. <https://doi.org/10.1016/j.energy.2021.120520>.
- [4] Gudmundsson O, Schmidt R-R, Dyrelund A, Thorsen JE. Economic comparison of 4GDH and 5GDH systems – using a case study. *Energy* 2022;238:121613. <https://doi.org/10.1016/j.energy.2021.121613>.
- [5] Lund H, Werner S, Wilshire R, Svendsen S, Thorsen JE, Hvelplund F, et al. 4th Generation District Heating (4GDH): integrating smart thermal grids into future sustainable energy systems. *Energy* 2014;68:1–11. <https://doi.org/10.1016/j.energy.2014.02.089>.
- [6] Lund H, Østergaard PA, Chang M, Werner S, Svendsen S, Sorknæs P, et al. The status of 4th generation district heating: research and results. *Energy* 2018;164:147–59. <https://doi.org/10.1016/j.energy.2018.08.206>.
- [7] Laajalehto T, Kuosa M, Mäkilä T, Lampinen M, Lahdelma R. Energy efficiency improvements utilising mass flow control and a ring topology in a district heating network. *Appl Therm Eng* 2014;69:86–95. <https://doi.org/10.1016/j.applthermaleng.2014.04.041>.
- [8] Hussam WK, Rahbari HR, Arabkoohsar A. Off-design operation analysis of air-based high-temperature heat and power storage. *Energy* 2020;196:117149. <https://doi.org/10.1016/j.energy.2020.117149>.
- [9] Rahbari HR, Arabkoohsar A, Jannatabadi M. Energy, exergy, economic and environmental analyses of air-based high-temperature thermal energy and electricity storage: impacts of off-design operation. *J Energy Resour Technol* 2021;143:070901. <https://doi.org/10.1115/1.4049453>.
- [10] Rahbari HR, Arabkoohsar A, Alrobaian AA. Thermodynamic, economic, and environmental analysis of a novel hybrid energy storage system: pseudo-dynamic modeling approach. *Int J Energy Res* 2021;45. <https://doi.org/10.1002/er.7077>. 20016–36.
- [11] Wang H, Hua P, Wu X, Zhang R, Granlund K, Li J, et al. Heat-power decoupling and energy saving of the CHP unit with heat pump based waste heat recovery system. *Energy* 2022;250:123846. <https://doi.org/10.1016/j.energy.2022.123846>.
- [12] Bergsteinnsson HG, Vetter PB, Møller JK, Madsen H. Estimating temperatures in a district heating network using smart meter data. *Energy Convers Manag* 2022;269:116113. <https://doi.org/10.1016/j.enconman.2022.116113>.
- [13] Sartor K, Dewalef P. Experimental validation of heat transport modelling in district heating networks. *Energy* 2017;137:961–8. <https://doi.org/10.1016/j.energy.2017.02.161>.
- [14] Betancourt Schwarz M, Mabrouk MT, Santo Silva C, Haurant P, Lacarrière B. Modified finite volumes method for the simulation of dynamic district heating networks. *Energy* 2019;182:954–64. <https://doi.org/10.1016/j.energy.2019.06.038>.
- [15] Wang H, Duanmu L, Lahdelma R, Li X. Developing a multicriteria decision support framework for CHP based combined district heating systems. *Appl Energy* 2017;205:345–68. <https://doi.org/10.1016/j.apenergy.2017.07.016>.
- [16] Wang H, Bo S, Zhu C, Hua P, Xie Z, Xu C, et al. A zoned group control of indoor temperature based on MPC for a space heating building. *Energy Convers Manag* 2023;290:117196. <https://doi.org/10.1016/j.enconman.2023.117196>.
- [17] Brown A, Foley A, Laverty D, McLoone S, Keatley P. Heating and cooling networks: a comprehensive review of modelling approaches to map future directions. *Energy* 2022;261. <https://doi.org/10.1016/j.energy.2022.125060>. 125060–125060.
- [18] Tesio U, Guelpa E, Verda V. Including thermal network operation in the optimization of a Multi Energy System. *Energy Convers Manag* 2023;277:116682. <https://doi.org/10.1016/j.enconman.2023.116682>.
- [19] Zheng X, Shi Z, Wang Y, Zhang H, Liu H. Thermo-hydraulic condition optimization of large-scale complex district heating network: a case study of Tianjin. *Energy* 2023;266:126406. <https://doi.org/10.1016/j.energy.2022.126406>.
- [20] Merlet Y, Baviere R, Vasset N. Optimal retrofit of district heating network to lower temperature levels. *Energy* 2023;282:128386. <https://doi.org/10.1016/j.energy.2023.128386>.
- [21] Guelpa E, Verda V. Compact physical model for simulation of thermal networks. *Energy* 2019;175:998–1008. <https://doi.org/10.1016/j.energy.2019.03.064>.
- [22] Gabrielaitiene I, Bøhm B, Sunden B. Evaluation of approaches for modeling temperature wave propagation in district heating pipelines. *Heat Tran Eng* 2008;29:45–56. <https://doi.org/10.1080/01457630701677130>.
- [23] Wang Y, You S, Zhang H, Zheng X, Zheng W, Miao Q, et al. Thermal transient prediction of district heating pipeline: optimal selection of the time and spatial steps for fast and accurate calculation. *Appl Energy* 2017;206:900–10. <https://doi.org/10.1016/j.apenergy.2017.08.061>.
- [24] Jie P, Tian Z, Yuan S, Zhu N. Modeling the dynamic characteristics of a district heating network. *Energy* 2012;39:126–34. <https://doi.org/10.1016/j.energy.2012.01.055>.
- [25] Chertkov M, Novitsky NN. Thermal transients in district heating systems. *Energy* 2019;184:22–33. <https://doi.org/10.1016/j.energy.2018.01.049>.
- [26] Price JF. Lagrangian and eulerian representations of fluid flow: kinematics and the equations of motion. 2006.
- [27] Steinegger J, Wallner S, Greiml M, Kienberger T. A new quasi-dynamic load flow calculation for district heating networks. *Energy* 2023;266:126410. <https://doi.org/10.1016/j.energy.2022.126410>.
- [28] Stevanovic VD, Zivkovic B, Prica S, Maslovacic B, Karamarkovic V, Trkulja V. Prediction of thermal transients in district heating systems. *Energy Convers Manag* 2009;50:2167–73. <https://doi.org/10.1016/j.enconman.2009.04.034>.
- [29] Zheng X, Shi K, Wang Y, You S, Zhang H, Zhu C, et al. Performance analysis of three iteration-free numerical methods for fast and accurate simulation of thermal dynamics in district heating pipeline. *Appl Therm Eng* 2020;178:115622. <https://doi.org/10.1016/j.applthermaleng.2020.115622>.
- [30] Toro EF. Riemann solvers and numerical methods for fluid dynamics: a practical introduction. Springer Verlag; 2009.
- [31] Benonysson A. Dynamic modelling and operational optimization of district heating systems. In: Laboratory of heating and air conditioning. Technical University of Denmark; 1991.
- [32] Stevanovic VD, Jovanovic ZLJ. A hybrid method for the numerical prediction of enthalpy transport in fluid flow. *Int Commun Heat Mass Tran* 2000;27:23–34. [https://doi.org/10.1016/S0735-1933\(00\)00081-6](https://doi.org/10.1016/S0735-1933(00)00081-6).
- [33] Wang H, Meng H. Improved thermal transient modeling with new 3-order numerical solution for a district heating network with consideration of the pipe wall's thermal inertia. *Energy* 2018;160:171–83. <https://doi.org/10.1016/j.energy.2018.06.214>.
- [34] Sartor K, Thomas D, Dewallef P. A comparative study for simulating heat transport in large district heating networks. *IJHT* 2018;36:301–8. <https://doi.org/10.18280/ijht.360140>.
- [35] Duquette J, Rowe A, Wild P. Thermal performance of a steady state physical pipe model for simulating district heating grids with variable flow. *Appl Energy* 2016;178:383–93. <https://doi.org/10.1016/j.apenergy.2016.06.092>.
- [36] Zheng J, Zhou Z, Zhao J, Wang J. Function method for dynamic temperature simulation of district heating network. *Appl Therm Eng* 2017;123:682–8. <https://doi.org/10.1016/j.applthermaleng.2017.05.083>.
- [37] Zhao H. Analysis, modelling and operational optimization of district heating systems. Technical University of Denmark; 1995.
- [38] 7-technologies n.d. <https://www.se.com/ww/en/brands/7-technologies/> (accessed May 6, 2023).
- [39] Gabrielaitiene I, Bøhm B, Sunden B. Modelling temperature dynamics of a district heating system in Naestved, Denmark—a case study. *Energy Convers Manag* 2007;48:78–86. <https://doi.org/10.1016/j.enconman.2006.05.011>.
- [40] Gabrielaitiene I. Numerical Simulation of a District Heating System with Emphases on Transient Temperature Behaviour 2011;9.
- [41] TRNSYS: Transient System Simulation Tool n.d. <http://www.trnsys.com/>.

- [42] TRNSYS 17: A transient system simulation program - Mathematical Reference. vol. 4. Solar Energy Laboratory, University of Wisconsin-Madison; 2009.
- [43] Dénarié A, Aprile M, Motta M. Heat transmission over long pipes: new model for fast and accurate district heating simulations. *Energy* 2019;166:267–76. <https://doi.org/10.1016/j.energy.2018.09.186>.
- [44] Dénarié A, Aprile M, Motta M. Dynamical modelling and experimental validation of a fast and accurate district heating thermo-hydraulic modular simulation tool. *Energy* 2023;282:128397. <https://doi.org/10.1016/j.energy.2023.128397>.
- [45] Schweiger G, Larsson P-O, Magnusson F, Lauenburg P, Velut S. District heating and cooling systems – framework for Modelica-based simulation and dynamic optimization. *Energy* 2017;137:566–78. <https://doi.org/10.1016/j.energy.2017.05.115>.
- [46] Oppelt T, Urbaneck T, Gross U, Platzer B. Dynamic thermo-hydraulic model of district cooling networks. *Appl Therm Eng* 2016;102:336–45. <https://doi.org/10.1016/j.applthermaleng.2016.03.168>.
- [47] 3 Operators and Expressions• Modelica® - A Unified Object-Oriented Language for Systems Modeling Language Specification Version 3.4 n.d. <https://specification.modelica.org/v3.4/Ch3.html> (accessed November 15, 2022).
- [48] van der Heijde B, Fuchs M, Ribas Tugores C, Schweiger G, Sartor K, Basciotti D, et al. Dynamic equation-based thermo-hydraulic pipe model for district heating and cooling systems. *Energy Convers Manag* 2017;151:158–69. <https://doi.org/10.1016/j.enconman.2017.08.072>.
- [49] Giraud L, Baviere R, Vallée M, Paulus C. Presentation, validation and application of the DistrictHeating. *Modelica Library*; 2015. p. 79–88. <https://doi.org/10.3384/ecp1511879>.
- [50] Klemm C, Wiese F, Vennemann P. Model-based run-time and memory reduction for a mixed-use multi-energy system model with high spatial resolution. *Appl Energy* 2023;334:120574. <https://doi.org/10.1016/j.apenergy.2022.120574>.
- [51] Robinson S. *Simulation: the practice of model development and use*. Hoboken, NJ: John Wiley & Sons, Ltd; 2004.
- [52] Capone M, Guelpa E, Verda V. Accounting for pipeline thermal capacity in district heating simulations. *Energy* 2021;219:119663. <https://doi.org/10.1016/j.energy.2020.119663>.